Iraqi National Journal of Chemistry

Journal homepage:
http://iqnjc.com/Default.aspx

# The photochemical Catalytic Properties and Hydrothermal Synthesis of Nano Bismuth Borate for Efficient Removal of Congo red dye from Aqueous Solution.

Hasan J. Mohammed[1], Zaki N. Kadhim[1]

[1] University of Basra, College of Science, Chemistry Department

Email: Jasiem33@gmail.com, zaki.kadhim@uobasrah.edu.iq

Abstract

This study synthesized Bismuth Borate (BB) by one-step precipitation from nano bismuth oxide and Boric acid. FTIR, XRD, SEM, EDX, and Zeta potential characterized the product. This product acts as a photocatalyst to remove Congo red dye (CR) from an aqueous solution, all factors that affect the adsorption process studied (Time, weight of adsorbent, adsorbate concentration, PH, temperature). Model of isotherm adsorption Langmuir and Freundlich, kinetic adsorption, first- and second-order pseudo and thermodynamic values (ΔS, ΔG, ΔH) are studied. Results of the study indicated that the best amount of adsorbent was 0.1 g used against dye, the optimal concentration of CR was 50 mg L-1, and the optimum acidity function was equal to 5.5 with a volume of 100 ml of aqueous solution. Adsorption processes were carried out using distilled water as solvent. Also, this study included calculating adsorption capacity based on optimal conditions obtained by applying Langmuir and Freundlich isotherm models and max = (196) mg g-1 for (BB), kinetic adsorption following second-order pseudo. Values of thermodynamics (ΔS, ΔG, ΔH) are measured, and the results indicate an increase in system randomness and that the adsorption process is spontaneous and endothermic.

**Keywords:** Hydrothermal, Bismuth Borate (BB), Congo red dye (CR), Adsorption.

## 1 Introduction

Bismuth borate is one of the compounds most frequently included in research studies because of its importance and distinctive properties, including composition and crystal structure, physical properties, chemical and thermal stability, high ability to block radiation, optical efficiency, and high surface area[1]. These properties have been exploited to apply these compounds in many industrial, medical, and research fields, including soil fertilization, semiconductor materials, infrared detection, and radiation dose measurement[2]. Substances are used to add color of all types and sources, whether liquid, solid, or solutions previously prepared by dissolving colored materials in suitable solvents[3]. These materials are either dyes or pigments, which come from a natural or artificial source. These colored materials are usually divided according to whether they are basic, acidic, organic, and inorganic[4]. These dyes are used in many industrial fields in coloring leather, papers, paints, inks, fabrics, and textiles[5]. They are also used in biological and analytical fields as reagents. Congo red dye is an organic synthetic dye that belongs to the azo dye family because it contains two azo rings in its chemical structure[6]. Congo red dye is used in

many coloring processes, requiring large amounts of water for dyeing. Therefore, no less than 15% of this dye leaks in surplus into streams, streams, rivers, and lakes, and thus it can also seep into the ground[7]. Continuation This leakage increases the concentration of this dye, leading to pollution of the aquatic environment, causing a change in the color of the water and a negative impact on plants and animals[8]. Additional danger of Congo red dye is represented by human safety, as it can cause problems with the urinary system, cirrhosis of the liver, skin inflammation, and eye allergies, as well as incurable diseases like cancer[9]. Preserving the aquatic environment is considered one of the priorities adopted by humans, as they directed and created various methods for treating wastewater. There are numerous theories, including separation, evaporation, and osmotic pressure. Adopting and working on one of these theories depends on several criteria, including cost, ease of application, time, safety, waste, and Availability of basic materials[10]. Adsorption is considered one of the methods of treating polluted water, as in this way, it is possible to exclude dyes or inorganic, organic molecules, salts, impurities, and target ions[11]. The adsorption process is easy to apply, low cost, a safe, good time to complete the process, and an environmentally friendly process that does not leave waste in large quantities, as it is possible to reactivate adsorbents[12]. Adsorbents come from multiple sources, including organic, inorganic, and polymer, and many are easy to prepare[13]. The principle of the adsorption process is based on the adhesion of molecules and ions of adsorbed materials, whether liquid or gaseous, to the surface and inside the pores of the adsorbent materials[14]. Therefore, adsorption is physical if the molecules of the adsorbent adhere to the adsorbent material employing electrostatic van der Waals forces; these forces are relatively weak, causing the adsorbent from adsorbate to separate, reversing the adsorption process. Therefore, this adsorption is called reversible, and the reversal of the adsorption process can be obtained by controlling the conditions of the adsorption process, such as pressure and temperature[15]; this type of adsorption does not require high activation energy, and it is multi-layered. Chemical adsorption occurs as a result of the presence of a connection through relatively strong chemical bonds between the adsorbent and the adsorbate; therefore, breaking this bond is relatively difficult; this type of adsorption is considered irreversible[16] It is characterized by being single-layer, and requires high activation energy. What distinguishes chemical adsorption is the high range of selectivity direction of molecules, ions, and atoms to be excluded and the abundance of raw materials involved in the adsorption process. The study aims to prepare Bismuth borate, which can act as a photocatalyst to remove Congo red day from aqueous solution by adsorption.

## Methods

### Preparing Adsorbent

Bismuth borate was synthesized by one-single-step precipitation by mixing bismuth oxide NP and boric acid in a molar ratio (3:1) in 200 ml distilled water under stirrer 500 rpm at mixing time for 10 hours at 60 0C. After that, the mixture was filtered and then washed several times with distilled water to remove the excess boric acid. The product dried in an oven for 24 hours at 70 0C.

### Preparing Adsorbate

Congo Red dye solution was prepared by dissolving 1 g of dye in 1000 ml of distilled water; after that, different concentrations of dye were prepared.

### Photocatalyst process

A different concentration of dye was prepared at pH (5.5) and at the required temperature and placed in a test tube. After that, adsorbent (BB) loaded with weight (0.1) g was placed in a shaker and exposed to sunlight for an interval of time. The aqueous solution was then centrifuged to separate it and measured at a wavelength of 495 nm.

## Results and discussion

### FTIR spectra

The obtained FTIR spectra of Bismuth borate are shown in Figure 1. The peak at 3448.48 $cm^{-1}$ is due to the O–H group in the bismuth borate. The peak at 1458.23 $cm^{-1}$ and the peak at 1388.79 $cm^{-1}$ belong to the asymmetric stretching of B(3)–O and in-plane bending of B–O–H, respectively. The peak at 844.85 cm-1 is a stretching vibration of B(4)–O. The peak at 551.66 $cm^{-1}$ is attributed to the in-plane bending of B(3)–O. The peak at 420 $cm^{-1}$ is due to the bending of Bi–O[17].

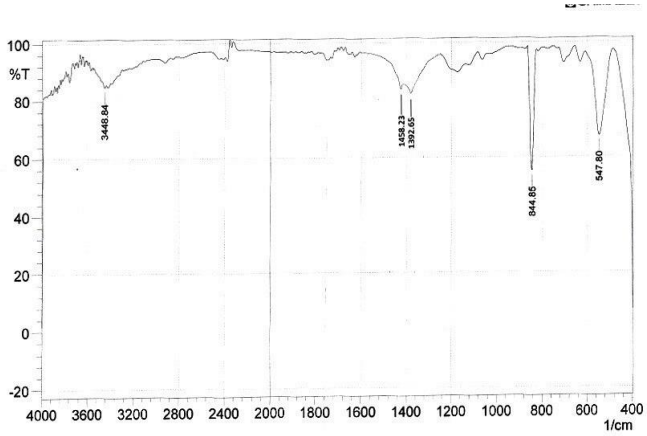


**Figure 1: FTIR spectra of Bismuth borate obtained at $60^0$ C**

### XRD analysis

XRD pattern of bismuth borate shown in Figure 2. Values of (2θ) for the main peaks of Bismuth borate were reported as 12.55°,23.95°, 28.03°,30.19°, 32.79°,42.00° ,46.32C , 46.06,47.06°, 55.62° and 56.9°[18]. Average crystallites size in (28.85) nm as calculated from Scherrer equation . that crystals of the compound fall within nanoscales .

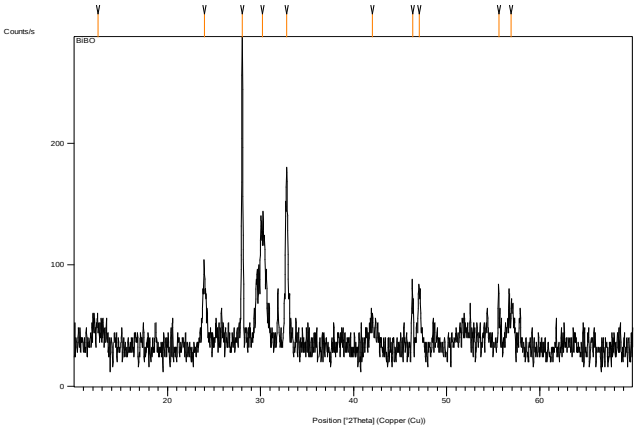


**Figure 3: XRD Patterns of Bismuth borate**

## SEM analysis

The shapes represent images of the scanning electron microscope with a field of light emission of the prepared compound, figures of the compound showed overlapping scales, and the surface of the compound contains holes and pores as shown in Figure 3(a-d). The presence of these pores increases the surface area of the compound. Therefore, these holes are important in increasing adsorption[19]. Average porose size in (77) nm.

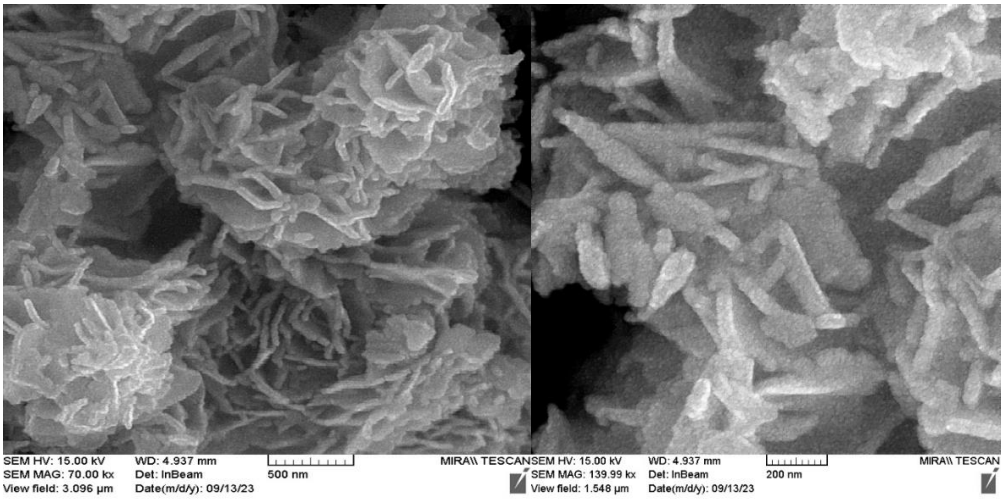


a b

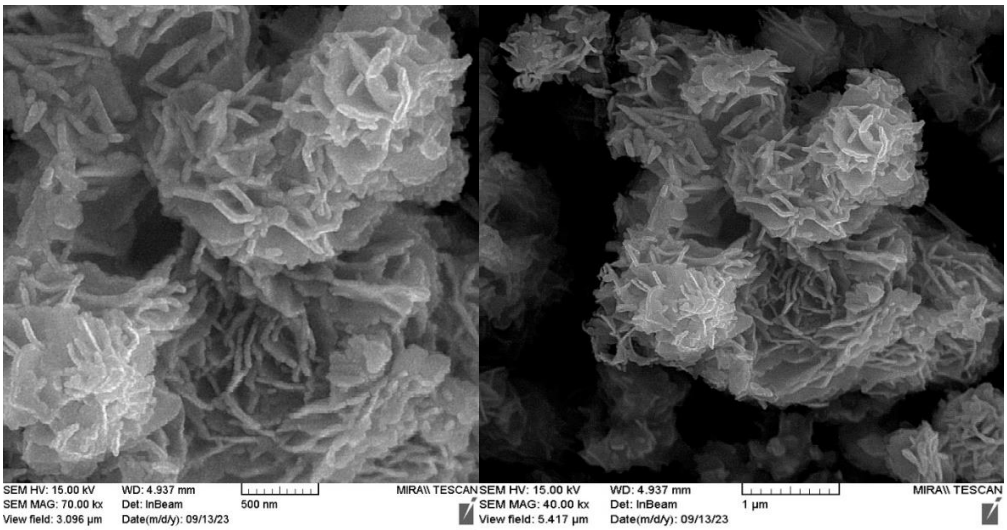


c d

**Figure 3(a-d) SEM of Bismuth borate**

## EDX analysis

Table 1 and Figure 4 show EDX analysis of bismuth borate. The chemical composition of the bismuth borate sample was determined as Bismuth 77.87%, oxygen 16.56%, and boron 5.57%, using data from EDX analysis[20]. This proves that the synthesis nano practical of BB is successfully.

**Table (1): EDX values of Bismuth borate composition.**

| Composition | W % | A % |
|---|---|---|
| B | 5.57 | 10.52 |
| O | 16.56 | 62.76 |
| Bi | 77.87 | 26.72 |
| Total | 100.00 | 100.00 |

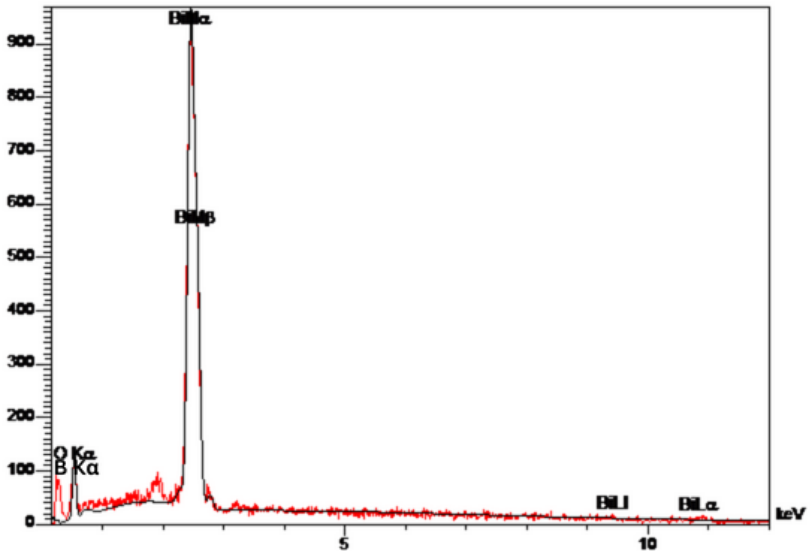


**Figure 4: EDX positions of Bismuth borate compound**

## Zeta potential analysis

There are many different ways of calculating zeta potential. In this study, method of calculating zeta potential in electrophoretic.

**Table (2): explain range of stability according to zeta potential.**

| Stability behavior of the particles | Zeta Potential (mV) |
|---|---|
| Rapid Coagulation or Flocculation | 0 to ±5 |
| Incipient Instability | ±10 to ±30 |
| Moderate Stability | ±30 to ±40 |
| Good Stability | ±40 to ±60 |
| Excellent Stability | More than ±61 |

As shown in Figure 5 and Table 3, the value of the zeta potential of bismuth borate ( -57.6 mv ) and that is means the surface of the product has a negative charge, and it is stable[21], and it is good to use to adsorb Congo red dye from aqueous solution. bismuth borate product, it is too difficult to make colloid with solution, so it is easy to isolate it from aquas solution.

**Table (3): zeta potential of Bismuth borate**

| Peak NO: | zeta potential | Electrophoretic |
|---|---|---|
| 1 | - 57.6 mV | 0.000298 $cm^2/Vs$ |

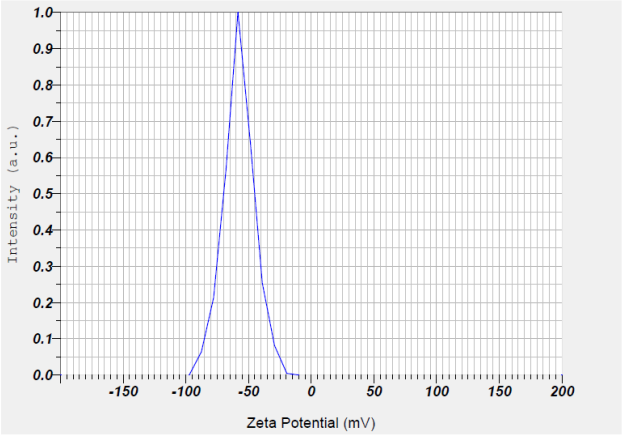


**Figure 5: Zeta potential position of (BB) surface**

**Determination the calibration curve.**

Standard curve of Congo red dye was calculated by preparing different concentrations 5,10,15,20,25 ppm at pH = 8 and the absorption was measured at the highest wavelength 495 nm by plotting concentration versus absorption, where $R^2$ = 0.9973 represents the linear equation as in Figure 6.

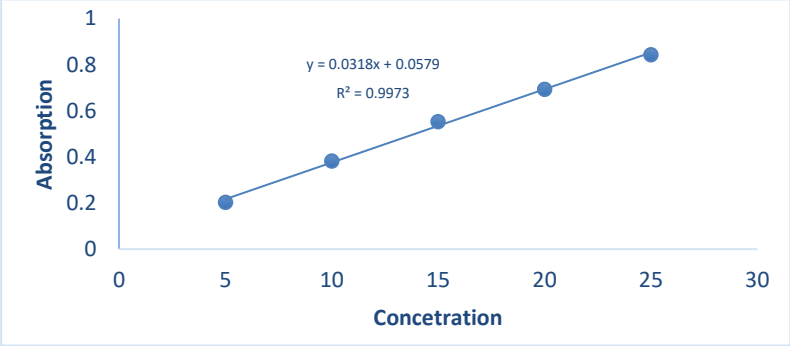


**Figure 6: stander curve of Congo red dye.**

**Adsorption studies**

**Study of adsorption time Equilibrium**

The factor affecting of adsorption efficiency is the equilibrium time between the adsorbent bismuth borate and Congo red dye. Using a weight of 0.1 gm with a dye concentration 25 ppm at a temperature 300 $^0$K at different times within the range 1-100 min, as the results shown in Figure 7 and Table 4 show that time of 30 min is best equilibrium time for adsorption process.

**Table (4): Equilibrium time of adsorption process.**

| $q_{(mg/g)}$ | 16.977 | 20.531 | 21.569 | 23.644 | 23.959 | 24.022 |
|---|---|---|---|---|---|---|
| Time (min) | 5 | 10 | 15 | 30 | 45 | 60 |

q: Amount of adsorbate on BB adsorbent in (mg/g)

$$q = \frac{(C_o - C_e)V}{M}$$

were

$C_0$ : initial concentration of CR in solution in (mg/L)

$C_e$ : Remaining concentration of CR in solution

V : Volume of solution in (L)

M: Wight of adsorbent (BB) in (g)

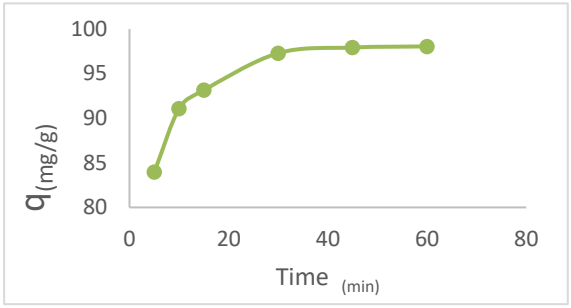


**Figure 7: effect change time on adsorption process .**

**Study of factors that affecting on percentage removal of CR dye from aqueous solution using (BB) as adsorbent.**

**Effect of adsorbent weight**

Effect of altering weight of adsorbent on adsorption process was studied using a weights 0.06,0.1,0.2,0.3, g and at times up to 60 min and dye concentration 25 ppm and volume 100 ml of aqueous solution and wavelength (495 nm) It was found that adsorption increases with increase catalyst weight due to increase in surface area that provides greatest value for the active areas[22] as shown in Table 5 and Figure 8.

**Table 5 amount of CR dye adsorbed on (BB) adsorbent in (mg/g)**

| Weight (g) | 0.06 | 0.1 | 0.2 | 0.3 |
|---|---|---|---|---|
| $(q)_{mg/g}$ | 7.921 | 15.405 | 21.915 | 23.707 |

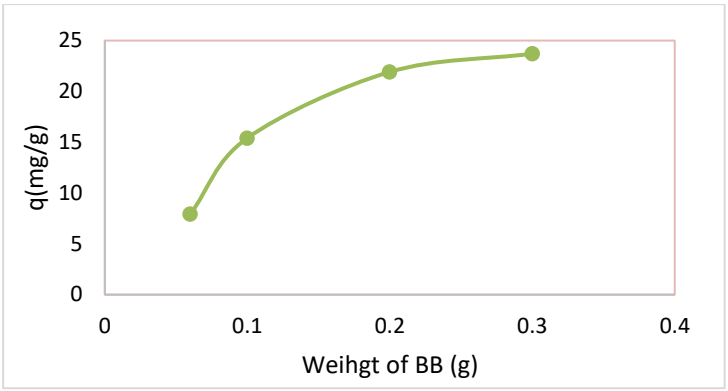


**Figure 8: effect change wight of (BB) adsorbent on adsorption process.**

## Effect of pH

Removal percentage of CR dye using 0.1 g of (BB) in 100 ml with 25 ppm at time 60 min with different pH 3,5,7,9,11, adsorption of dye in acidic medium is greater than in base medium[23] as shown in Table 6 and Figure 9, ability of dye tendency to bind in acidic medium with catalyst is more than its tendency to bind with solvent molecules, since process of remove dye by photocatalysis is subject to several mechanisms, including direct reduction by electrons in the conduction beam, direct oxidation through gaps in the valence beam, and finally hydroxy radical attack. These mechanisms mentioned depend on nature of material and pH function of medium in which adsorption process takes place has an effect on both adsorbate and adsorbent. But it should be noted that this dye is deposited at pH=2 and also changes the color of dye at acid function pH=3 causing a difference in wavelength, so it was settled to use value of pH = 5.5 in next experiments.

**Table (6): Effect pH on adsorption process.**

| pH | 3 | 5 | 7 | 9 | 11 |
|---|---|---|---|---|---|
| q | 24.493 | 18.141 | 13.158 | 11.128 | 12.135 |

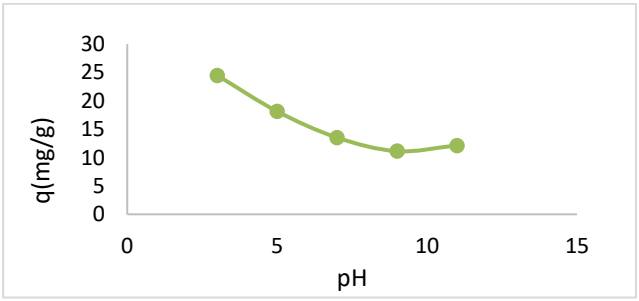


**Figure 9: effect of change pH solution on the adsorption process.**

## Effect of Initial dye Concentration

The altering concentration of dye affects the adsorption process, which is one of the important factors, so in this study, different concentrations of Congo red dye were taken. Values 50,75,100,125 and 150 ppm with a constant weight of adsorbent of Bismuth borate, an increase in adsorption efficiency was observed with increased concentrations of dye where the highest adsorption value was recorded[24] as shown in Table 7. This is due to the fact that largest amount of dye will be adsorbed on adsorbent and thus, the generation of free radicals for hydroxyl will decrease due to lack of active sites of hydroxyl ions, noting a decrease in percentage of adsorption in high initial concentration of dye, which hinders access of photons of light to the catalytic surface causing a decrease in absorption of photons[25]consequently a decrease in decomposition rate.

**Table 7 effect of Initial dye Concentration On adsorption process.**

| $C_0$ (ppm) | 50 | 75 | 100 | 125 | 150 |
|---|---|---|---|---|---|
| q (mg/g) | 34.819 | 48.863 | 63.956 | 76.667 | 89.384 |

**Table 8 Maximum adsorption at a maximum concentration of CR dye**

| Adsorbent | BB |
|---|---|
| Concentration of CR dye (ppm) | 150 |
| q (mg/g) | 89.384 |

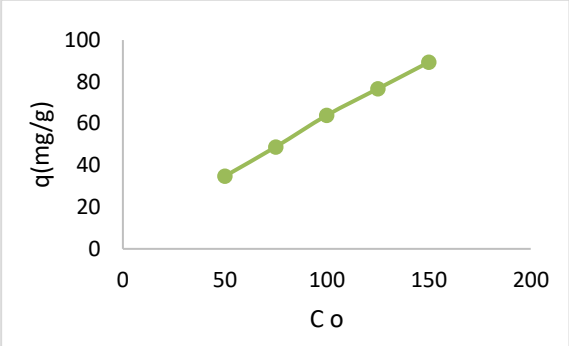


**Figure 10:** effect change of Initial dye Concentration on adsorption process**.**

## Effect of Temperature

Temperature of medium that occurs when adsorption is one of the factors effecting on removal dye, in this study the measurements were made at three temperatures ($300^0$K,$318^0$K and $333^0$K) where it was found that efficiency of adsorption increases with increasing temperature degree and accelerates access to equilibrium time[26] where the measurements made at a constant concentration and different times extended from (5-90 min), also the weight of adsorbent used to adsorb CR dye was constant 0.1 g, increasing efficiency of adsorption due to obstruction of the rearrangement electron - gap process due to increasing temperature, and this cycle proves that the adsorption process on this adsorbent is an endothermic process[27] in addition to that high

temperature increases rate of oxidation of organic compounds and thus enhances decomposition capacity. As shown in the Table 9 and Figure 11.

**Table (9): Effect of Change temperature on adsorption process.**

| Time(min) | 300 $^0$K | | 318 $^0$K | | 333 $^0$K | |
|---|---|---|---|---|---|---|
| BB | Ce | q | Ce | q | Ce | q |
| 5 | 8.022 | 41.97 | 11.73 | 38.26 | 7.393 | 42.60 |
| 10 | 4.468 | 45.53 | 3.871 | 46.12 | 2.833 | 47.16 |
| 15 | 3.430 | 46.56 | 3.116 | 46.88 | 2.298 | 47.70 |
| 30 | 1.355 | 48.46 | 1.827 | 48.17 | 1.198 | 48.80 |
| 45 | 1.040 | 48.95 | 1.386 | 48.16 | 1.103 | 48.89 |
| 60 | 0.726 | 49.27 | 1.292 | 48.70 | 0.726 | 49.27 |

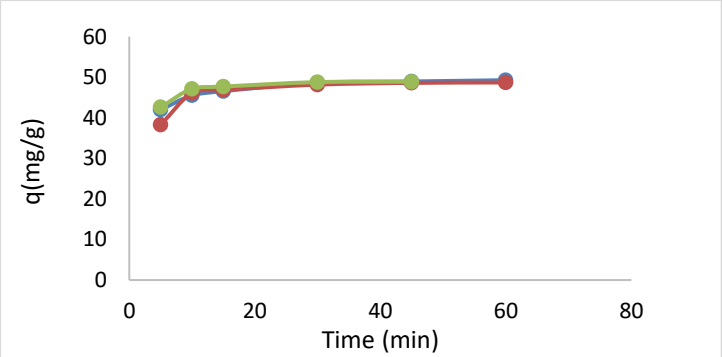


**Figure 11: effect change of temperature on adsorption process.**

## Adsorption Isotherm

Calculations and study of adsorption isotherm, calculations of effect primary dye concentration at room temperature 300$^0$K was used to apply the mathematical equation of isotherm Langmuir by plotting linear equation of Langmuir equation based on values of $C_e$ and Ce/qe as shown in Table 10 and Figure 12 Langmuir constant ($K_L$), values of maximum adsorption ($Q_{max}$) and correlation coefficient ($R_2$) were calculated, and these values are shown in Table 11.

**Table (10): Langmeyer isotherm study of adsorption**

| $C_0$ | $C_e$ | $q_e$ | $C_e/q_e$ |
|---|---|---|---|
| 50 ppm | 15.180 | 34.819 | 0.4359 |
| 75 ppm | 26.136 | 48.863 | 0.5349 |
| 100 ppm | 36.044 | 63.956 | 0.5635 |
| 125 ppm | 48.332 | 76.667 | 0.6304 |
| 150 ppm | 60.615 | 89.384 | 0.6781 |

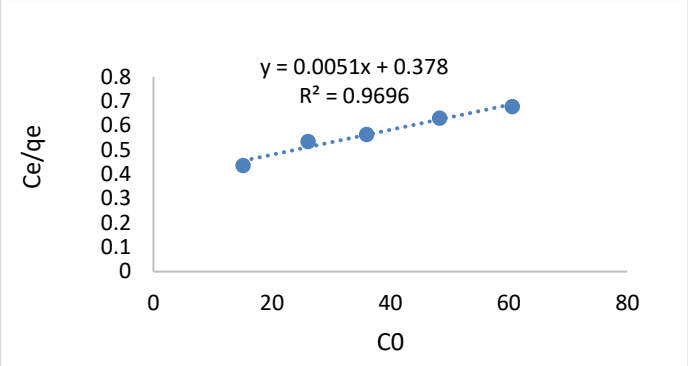


**Figure 12: Langmeyer adsorption Isotherm .**

**Table 11 Langmeyer constant ($K_L$), maximum value of adsorption (q max) and correlation coefficient ($R^2$)**

| Compound | $q_{max}$ | $K_L$ | $R^2$ |
|---|---|---|---|
| BB | 196 | 0.0135 | 0.9696 |

Linear relationship of Freundlich equation was plotting based on values of log Ce versus log $q_e$ shown in Table 12 and Figure 13.Values of Freundlich constants (R2,n,Kf) shown in Table 13 .

**Table (12): Freundlich's adsorption Isotherm**

| $C_0$ | 50 | 75 | 100 | 125 | 150 |
|---|---|---|---|---|---|
| Log $C_e$ | 1.1813 | 1.4172 | 1.5568 | 1.6842 | 1.7825 |
| Log $q_e$ | 1.5418 | 1.6889 | 1.8058 | 1.8846 | 1.9512 |

**Table (13): Freundlich's adsorption Isotherm values**

| Compound | Temp | n | $K_f$ (mg/g) | $R^2$ |
|---|---|---|---|---|
| BB | 300 k | 1.45 | 2.0632 | 0.9978 |

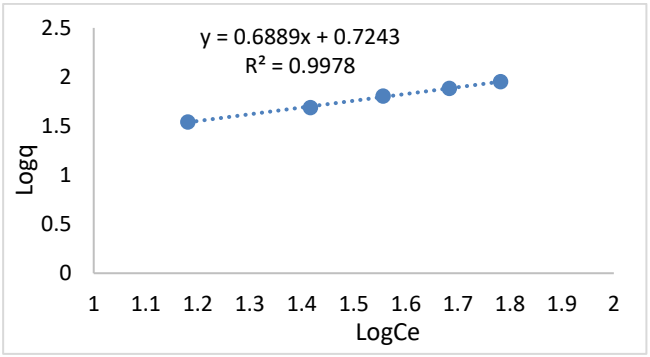


**Figure 13: Freundlich adsorption Isotherm .**

values $R^2 = 0.9696$ of Langmuir isotherm and $R^2 = 0.9978$ value of Freundlich Isotherm so that adsorption process flowing Freundlich isotherm model .

**Thermodynamic study calculation of thermodynamic functions.**

Through courante study effect of change temperature on the adsorption process, this helped to calculate thermodynamic functions (ΔH enthalpy, ΔG free energy and ΔS entropy).For adsorption of Congo red dye on adsorbent of Bismuth borate the importance of these functions to understanding adsorption process. Table 14 represents values of both ln kc and values of temperature , while Figure 14 represents relationship between ln Kc versus inverse of time (1/T), from which the values of (ΔH, (ΔS) can be obtained that can be calculated through values of interception = (ΔH/R) and slop= (ΔS/R), Table 15 shown thermodynamic values

**Table (14): values both (ln $k_c$) and values of Inverse temperature**

| $T(^0K)$ | 300 | 318 | 333 |
|---|---|---|---|
| $1/T * 10^{-3}$ | 3.333 | 3.144 | 3.003 |
| Ln $K_c$ | 2.068 | 2.711 | 2.821 |

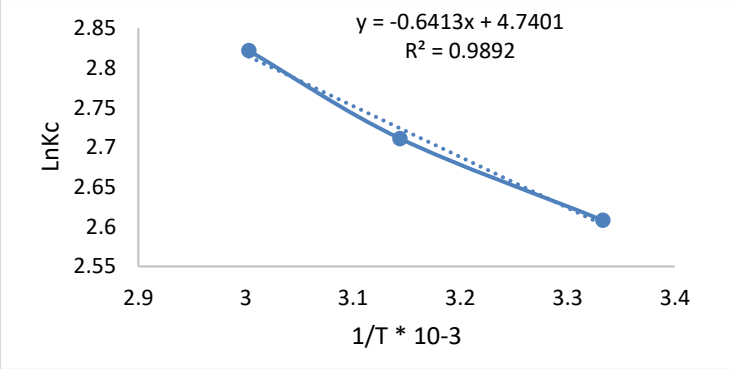


**Figure 14 Linear relationship between ln$k_c$ vs. $1/T*10^{-3}$ .**

**Table (15): values of (ΔH enthalpy, ΔG free energy ,ΔS entropy).**

| ΔG(KJ.mol$^{-1}$) | | | ΔS(KJ.K$^{-1}$.mol$^{-1}$) | ΔH(KJ.mol$^{-1}$) |
|---|---|---|---|---|
| 300 | 318 | 333 | | |
| -(33.85) | -(7.167) | -(7.811) | 39.41 | 5.331 |

From values shown above in Table 15 we conclude, free energy values ΔG of adsorption process all negative, which is evidence that adsorption process is spontaneous[28]. Entropy value ΔS for adsorption process positive , indicating that adsorbent molecules are in continuous motion on surface of adsorbent compound, indicating an increase in system randomness[29]. Value of enthalpy ΔH is positive for adsorption, indicating that adsorption process is endothermic[30] and that increase temperature leads to increase rate of propagation speed of adsorbed particles on adsorbent surface between pores in the adsorbent surface.

## Kinetic study

### False first order equation (Lagergren)

where the experimental data were applied to the Lagergren Pseudo first order equation Table 16 shown value of ln qe-qt and time values (t) of adsorption process and Figure 13 represent linear relationship of false first-order equation, from which adsorption rate constant ($K_1$), adsorption capacity ($q_e$) and correlation coefficient shown in Table 17 were calculated.

**Table (16) values of (ln qe-qt) versus the time values of the adsorption process.**

| Time (min) | 5 | 10 | 15 | 30 | 45 | 60 |
|---|---|---|---|---|---|---|
| $q_t$ | 41.977 | 45.531 | 46.569 | 48.644 | 48.959 | 49.273 |
| $q_e$ | 49.273 | 49.273 | 49.273 | 49.273 | 49.273 | 49.273 |
| log $q_e$-$q_t$ | 1.987 | 1.319 | 0.994 | -0.463 | -1.156 | NUM |

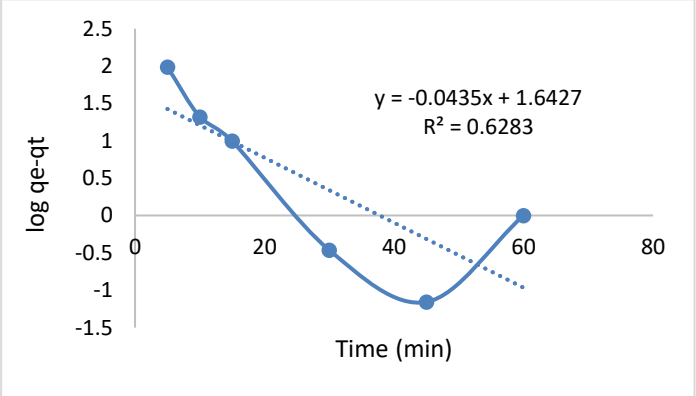


**Figure 15 linear relationship of false first-order equation.**

**Table (17): adsorption capacity ($q_e$) and the correlation coefficient**

| Comp | $Q_{e\,,\,exp}$ | $K_1(min^{-1})$ | $q_e$ (mg/g) | $R^2$ |
|---|---|---|---|---|
| BB | 49.273 | 0.000725 | 5.169 | 0.6283 |

### False second order equation

This equation shows that the adsorption rate depends on the adsorption amplitude in the adsorption surface, (Pseudo second order – equation).

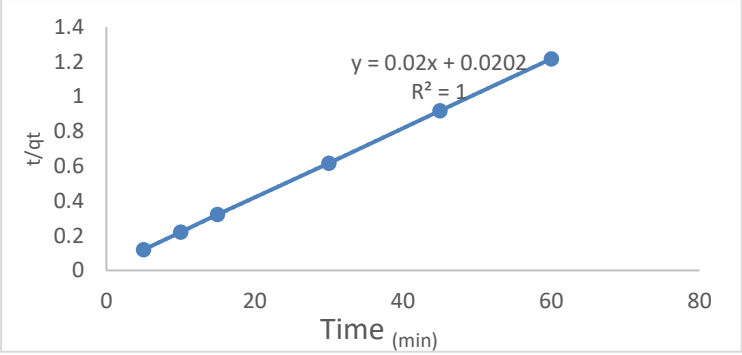


**Figure 16: linear relationship of the false second-order equation.**

**Table (18): adsorption capacity ($q_e$) and the correlation coefficient .**

| Compound | $Q_{e\ ,\ exp}$ | $K_2$ ($min^{-1}$) | $q_e$ (mg/g) | $R^2$ |
|---|---|---|---|---|
| BB | 49.273 | 0.0198 | 50 | 1 |

Values in Table 17 and Table 18 it is clear that process of adsorption following second kinetic equation for the reasons, the large difference between values of adsorption capacity calculated according to the false first order equation $qe_{(calculation)}$ is different from the experimental adsorption value $qe_{(experimental)}$ obtained through this study, as shown in Figure 15 linear axis of false first-order equation does not pass through all points, unlike linear axis of the false second-order equation, which passes exactly all points as shown in (Fig. 16). The correlation values R2 of the false first order equation is less than 0.8986 away from the value of 1 unlike the correlation value of $R^2$ of the false second-order equation, which is limits 0.999.

## Conclusions

Bismuth Borate successfully synthesized by one step precipitation from nano Bismuth oxide and Boric acid. FTIR spectra showed position of active aggregates of the compound. XRD analysis position of 2Θ for crystal lattice patterns proved formation of crystal. SEM analysis images of compound contains holes and pores. EDX analysis of solid product Bismuth borate sample was determined. Zeta potential analyses surface it is stable. All conditions effect on adsorption process have been study also isotherm and kinetic have been explained.

## الاستنتاجات

تم بنجاح تحضير بورات البزموث النانوية بالطريقة الحرارية المائية و بخطوة ترسيبية واحدة من خلال تفاعل اوكسيد البزموث النانوي مع حامض البوريك. تم تشخيص المركب بمطيافية الاشعة التحت الحمراء و التي اضهرت المواقع الفعالة للمركب التي تتطابق مع ظروف تفاعل التحظير من درجة حرارة و ضغط و حامضية . مطيافية الاشعة السينية المشتتة اضهرت مواقع (2 التي فسرت بنية الخلية للبلورة . صور المجهر الالكتروني الماسح بينت بوضوح وجودو مسامات و فجوات مناسبة theta ) الحجم لامتزاز صبغة الكونغو الاحمر من محلولها المائي . مطيافية الطاقة المشتتة بين النسب المئوية للعناصر الرئيسية المكونة للمركب حيث كانت النتائج بالقيم المطلوبة . قياس طاقة زيتا لسطح المركب كشف ان الشحنة للسطح هي سالبة و التي تفسر سبب عملية الامتزاز. جميع الظروف التي تؤثر على عملي الامتزاز تم دراستها كذلك حركية الامتزاز و نوعة.

## References


1. Sallam, O; Madboul, A; Elalaily, N; et al. Physical properties and radiation shielding parameters of bismuth borate glasses doped transition metals, Journal of Alloy sand Compounds, 2020; 843, 156056.
2. Sengupta, P. Environmental and occupational exposure of metals and their role in male reproductive functions. Drug and chemical toxicology, 2013; 36: 353-368.
3. Aguirre, CI; Reguera, E; Stein, A. Tunable colors in opals and inverse opals photonic crystals. Advanced Functional Materials. 2010; 20, 2565-2578.
4. Gürses, A; Güneş, K; Şahin, E. Removal of dyes and pigments from industrial effluents. In Green chemistry and water remediation. Research and applications, 2021; 135-187.
5. Benkhaya, S; M'rabet, S; El Harfi, A. A review on classifications, recent synthesis, and applications of textile dyes. Inorganic Chemistry Communications. 2020; 115, 107891.
6. Schmidt, C; Berghahn, E; Ilha, V. et al. Biodegradation potential of Citrobacter cultures for the removal of amaranth and congo red azo dyes. International Journal of Environmental Science and Technology, 2019; 16, 6863-6872.
7. Sarker, B; Keya, K; Mahir, F I; Nahiun, K M. et al. Surface and ground water pollution: Causes and effects of urbanization and industrialization in South Asia. Scientific Review. 2021; 7, 32-41.
8. Alsukaibi, AK. Various approaches for the detoxification of toxic dyes in wastewater. Processes. 2022; 10,1968.
9. Van Dorpe, I. Abstracts presented at the 20th Annual Congress of the Belgian Society of Internal Medicine: 11–12 December 2015, Brussels. Acta Clinica Belgica. 2015; 70, 1-41.
10. Warsinger, DM; Chakraborty, S; Tow, EW. et al. A review of polymeric membranes and processes for potable water reuse. Progress in polymer science, . 2018; 81, 209-237.
11. Velusamy, S; Roy, A; Sundaram, S. et al. A review on heavy metal ions and containing dyes removal through graphene oxide-based adsorption strategies for textile wastewater treatment. The Chemical Record, . 2021; 21, 570-1610.
12. Wang, L; Shi, C; Pa, L. et al. Rational design, synthesis, adsorption principles and applications of metal oxide adsorbents: a review. Nanoscale. . 2020; 12, 4790-4815.
13. Sabzehmeidani, MM; Mahnaee, S; Ghaedi, M. et al. Carbon-based materials: A review of adsorbents for inorganic and organic compounds. Materials Advances. (2021; 2, 598-627.
14. Alaqarbeh, M. Adsorption phenomena: definition, mechanisms, and adsorption types: short review. RHAZES: Green and Applied Chemistry. 2021; 13, 43-51.
15. Tomul, F; Arslan, Y; Kabak, B. et al. Adsorption process of naproxen onto peanut shell-derived biosorbent: important role of n–π interaction and van der Waals force. Journal of Chemical Technology & Biotechnology. . 2021; 96, 869-880.
16. Liu, J; Wei, Y; Li, P. et al. Selective H2S/CO2 separation by metal–organic frameworks based on chemical-physical adsorption. The Journal of Physical Chemistry. . (2017; C 121, 13249-13255.
17. Thakur, S; Thakur, V; Kaur, A. et al. Structural, optical, and thermal properties of nickel doped bismuth borate glasses. Journal of Non-Crystalline Solids. 2019; 512, 60-71.
18. Ghanem, AH; Farag, ATM; Al-Sehemi, AG. et al. Bismuth borate glass based nuclear materials. Silicon 10:1195-1201.
19. Natarajan S, Bajaj HC, Tayade RJ (2018) Recent advances based on the synergetic effect of adsorption for removal of dyes from wastewater using photocatalytic process. Journal of Environmental Sciences. 2018; 65, 201-222.

20. Xia, L; Xiao, Q; Ye, X. Erosion behavior and luminescence properties of Y3Al5O12: Ce3+-embedded calcium bismuth borate glass-ceramics for WLED s. Journal of the American Ceramic Society. 2019; 102, 2053-2065.
21. Kaur, P; Singh, KJ; Thakur, S. Investigation of bismuth borate glass system modified with barium for structural and gamma-ray shielding properties. Spectrochimica Acta Part A: Molecular and Biomolecular Spectroscopy, 2019; 206, 367-377.
22. Egbosiuba, TC; Abdulkareem, AS; Kovo, AS. Ultrasonic enhanced adsorption of methylene blue onto the optimized surface area of activated carbon: Adsorption isotherm, kinetics, and thermodynamics. Chemical engineering research and design. 2019; 153, 315-336.
23. Mittal, A; Mittal, J; Malviya, A; et al. Adsorptive removal of hazardous anionic dye "Congo red" from wastewater using waste materials and recovery by desorption. Journal of colloid and interface science. 2009; 340, 16-26.
24. Rajabi, HR; Arjmand, H; Kazemdehdashti, H. et al. A comparison investigation on photocatalytic activity performance and adsorption efficiency for the removal of cationic dye: quantum dots vs. magnetic nanoparticles. Journal of environmental chemical engineering. 2016; 4, 2830-2840.
25. Reza, KM; Kurny, ASW; Gulshan, F. Parameters affecting the photocatalytic degradation of dyes using TiO 2: a review. Applied Water Science. 2017; 7, 1569-1578.
26. Lyu, Z; Shen, A; He, Z. et al. Absorption characteristics and shrinkage mitigation of superabsorbent polymers in pavement concrete. International Journal of Pavement Engineering. 2022; 23, 270-284.
27. Kasera, N; Kolar, P; Hall, SG. Nitrogen-doped biochars as adsorbents for mitigation of heavy metals and organics from water: A review. Biochar. 2022; 4, 17.
28. Wang, B; Zhang, Q; Xiong, G. et al. Bakelite-type anionic microporous organic polymers with high capacity for selective adsorption of cationic dyes from water. Chemical Engineering Journal. 2019; 366, 404-414.
29. He, J; Guo, J; Zhou, Q. et al. Analysis of 17α-ethinylestradiol and bisphenol A adsorption on anthracite surfaces by site energy distribution. Chemosphere. 2019; 216, 59-68.
30. Fatombi, JK; Idohou, EA; Osseni, SA. et al. Adsorption of indigo carmine from aqueous solution by chitosan and chitosan/activated carbon composite: kinetics, isotherms, and thermodynamics studies. Fibers and Polymers. 2019; 20, 1820-1832.